New Journal of Physics
The open-access journal for physics

# Positron collisions with Rydberg atoms in strong magnetic fields

**P H Donnan and F Robicheaux**[1]
Department of Physics, Auburn University, AL 36849-5311, USA
E-mail: robicfj@auburn.edu

*New Journal of Physics* **14** (2012) 035018 (15pp)
Received 22 November 2011
Published 28 March 2012
Online at http://www.njp.org/
doi:10.1088/1367-2630/14/3/035018

**Abstract.** We have calculated the rates for the processes that result from collisions of positrons with Rydberg atoms in strong magnetic fields. This is the first step in a two-stage charge transfer, which is being explored as a mechanism for the formation of cold anti-hydrogen. Unlike previous theoretical explorations we have also investigated the cases when the energy of the positrons can be comparable to or larger than the binding energy of the atom. We have also examined how big an electric field is needed to destroy the resulting positronium. We find that the charge transfer does not scale as $\sqrt{T}$ for $n = 40$ states for positron temperatures above $T \sim 25$ K. Also, we find that the positronium atoms are more easily destroyed by electric fields if they emerge from the charge transfer along the magnetic field lines, contrary to what might be expected for the $\vec{v} \times \vec{B}$ effective electric field. Both results have implications for the formation of anti-hydrogen atoms.

[1] Author to whom any correspondence should be addressed.

## Contents



## 1. Introduction

Experiments performed by the ALPHA collaboration have recently demonstrated the ability to trap anti-hydrogen [1] and to hold the atoms for more than 15 min [2]. The ALPHA collaboration caused cold anti-protons, $\bar{p}$'s, to traverse a cold positron, $e^+$, plasma [3]; a $\bar{p}$ can capture one of the $e^+$'s during its brief time in the plasma, leading to the formation of highly excited anti-hydrogen atoms, $\bar{H}$'s. Presumably, the $\bar{H}$'s are mainly formed through three-body capture [4–6] since this mechanism has the largest rate for the parameters of the experiments. In three-body capture, $e^+$'s scatter in the field of a $\bar{p}$ so that a $e^+$ loses enough energy to become bound to the $\bar{p}$. The neutral $\bar{H}$'s can be trapped using their magnetic moment. Taking the Bohr magneton times a 1 T magnetic field change as the unit of energy gives a well depth of $\sim 2/3$ K. This small well depth, compared to the temperatures of the plasmas and the energies through which the $\bar{p}$'s need to be excited to reach the $e^+$ plasma, leads to a small fraction of the $\bar{H}$'s getting trapped.

The work reported here is a set of calculations important for a different method from the one above for the formation of $\bar{H}$. This method was suggested in [7] and uses a two-stage charge transfer to attach the $e^+$ to the $\bar{p}$. They proposed that a beam of Rydberg atoms be directed through a $e^+$ plasma that is close to trapped $\bar{p}$'s. When the Rydberg atom enters the $e^+$ plasma, a charge exchange quickly occurs, giving a highly excited positronium (Ps). A fraction of the Ps population travels to the region of the trapped $\bar{p}$'s where a second charge exchange can occur. These reactions can be summarized as

$$e^+ + Ry^* \rightarrow Ry^+ + Ps^* \quad \text{and} \quad Ps^* + \bar{p} \rightarrow e^- + \bar{H}^*. \tag{1}$$

Because the kinetic energy of the $\bar{H}$ is mostly determined by the kinetic energy of the $\bar{p}$ just before charge exchange, the $\bar{H}$ formed in the two-stage charge exchange could be moving less rapidly than that formed by three-body capture of the one-stage method used in [1, 2]. Thus, a two-stage charge transfer might lead to a larger fraction of trapped $\bar{H}$'s. The ATRAP collaboration reported a successful implementation [8] of this two-stage charge transfer method for $\bar{H}$ formation, but have not reported results on attempts to trap the $\bar{H}$'s formed with this method.

The two-stage charge transfer was simulated including the strong magnetic field [9] with the intention of understanding the properties of the Ps formed in the first step and the properties of the resulting $\bar{H}$'s. Wall *et al* [9] found that the Ps tended to emerge from the first charge exchange with a nearly isotropic distribution with a formation rate of

$$\langle v\sigma\rangle(n, T, B) \equiv C(n, T, B)(2n^2a_0)^2\sqrt{k_B T/m}, \tag{2}$$

where $C$ is a dimensionless constant, $n$ is the principal quantum number of the Rydberg atom, $T$ is the temperature of the $e^+$ plasma, $B$ is the magnetic field, $k_B$ is Boltzmann's constant and $m$ is the mass of the $e^+$. The formation rate times the $e^+$ plasma density gives the rate (in $s^{-1}$) for the conversion of the Rydberg atom into a highly excited Ps. Calculations were performed for $n = 30, 40, 50$, $B = 1, 2, 4$ T and temperatures of 4 and 8 K. The rate coefficient $C$ was reported to be in the range $4 < C < 6.5$ for all of the $n$, $T$ and $B$ combinations investigated. For the case $B = 0$, one can use classical scaling to show that the $C$ will only depend on the combination $n^2T$. The value of $C$ from [9] gives results comparable to the 'velocity-averaged' cross section of $9.7\pi n^4 a_0^2$ found in [7] for zero magnetic field.

Almost all of the highly excited Ps will travel to the $\bar{p}$ without changing their principal quantum number due to the emission of photons. A typical Ps center-of-mass speed is several $10^4$ m s$^{-1}$ and the distance to the $\bar{p}$ is a few cm; this gives $\mu$s as the relevant time scale between the two charge transfers, which is too short for a substantial probability for the highly excited Ps to emit a photon or simply annihilate. Because almost all of the Ps survive to the distance where the second charge exchange can occur, the possibility for the second charge exchange only depends on the cross section for the second exchange and the angular distribution of the Ps as they emerge from the first exchange. For example, an isotropic distribution leads to the number of $\bar{H}$'s being

$$N_{\bar{H},\mathrm{iso}} = N_{\mathrm{Ps}} N_{\bar{p}} \frac{\sigma}{4\pi R^2}, \tag{3}$$

where $N_{\mathrm{Ps}}$ is the number of Ps formed, $N_{\bar{p}}$ is the number of $\bar{p}$'s in the trap, $R$ is the distance between where the Ps forms and the $\bar{p}$'s are trapped, and $\sigma$ is the charge transfer cross section of the $e^+$ of the Ps to the $\bar{p}$ to form $\bar{H}$. The charge transfer cross section is a few times the geometrical cross section which is $\pi(2n^2a_0)^2$. For $n = 40$ and $R = 5$ cm, the ratio of the cross section to the surface area, $\sigma/(4\pi R^2) \sim 10^{-11}$. Using the expression for $N_{\bar{H},\mathrm{iso}}$, this means that 1 million Ps formed in a trap containing 1 million $\bar{p}$'s will lead to only $\sim$10 $\bar{H}$'s formed. If the Ps angular distribution were more aligned along the magnetic field, then more $\bar{H}$'s would be formed with the same number of Ps because the $\bar{p}$ plasma and the $e^+$ plasma are aligned along the same axis.

When the simulations were performed for [7, 9], it was thought that the temperature of the positron plasma would be comparable to the temperature of the trap, $\sim$4 K. However, it is now known that the octupole or quadrupole fields used to trap the $\bar{H}$'s cause the positron plasmas to substantially heat up unless the plasma has a very small radius and length. This heating can occur because the octupole or quadrupole breaks the cylindrical symmetry, which allows the plasmas to expand more quickly; the expansion decreases the electric potential energy with the resulting energy released as heat into the plasma. Thus, we have now simulated the first charge transfer step with higher temperature $e^+$'s. If the plasma temperature becomes comparable to the binding energy of the Rydberg atom, then the charge transfer process becomes modified by the higher speed of the $e^+$ and ionization can occur. As an indication of the energy scales involved, a Rydberg atom in the $n = 40$ state has a binding energy of $\sim$100 K. Another limitation of [7, 9]

was that a new atom geometry was generated for each $e^+$ launched at the atom; thus, every $e^+$ collision was for an atom with the same binding energy. However, in the plasma, there will be many $e^+$-atom collisions before ionization or charge transfer occurs. We performed calculations where we fired a thermal distribution of $e^+$ at the atom to see what effect this had on the Ps properties. For these calculations, each successive $e^+$ can change the binding energy and angular momentum of the atom; we fire $e^+$'s at the atom until it is ionized or a charge transfer occurs. Finally, the Ps are formed in a trap where electric fields in the 10–100 $\mathrm{V\,cm^{-1}}$ range occur. Thus, it is interesting to compute what strength of electric fields the Ps can survive and how this survival probability depends on the direction that the Ps travel relative to the $B$-field.

The question of which principal quantum number of the Rydberg atom most effectively leads to trapped $\bar{H}$ atoms is complicated because two trends lead to opposite behavior. The first trend is that the binding energy of the atom directly affects the formation rate of the Ps, the binding energy of the Ps and the cross section of the second charge transfer. The binding energy of the Ps is comparable to the original binding energy of the Rydberg atom if the $e^+$ is cold; thus, the second charge transfer cross section tends to increase with $n$. More $\bar{H}$'s presumably would lead to more trapped atoms. Other trends work against this effect. For example, if the original atom is less weakly bound, then the $e^+$ may tend to ionize the atom before charge transfer occurs, which will tend to decrease the number of Ps formed. Another example is that the weakly bound Ps might be destroyed by the $E$-fields in the trap. Finally, as shown in [9], as $n$ increases, the fraction of atoms that are in the low field seeking states tends to decrease.

As was done in [7, 9], we use a classical trajectory Monte Carlo method to compute the properties of the Ps. This should be an accurate method because the states that are involved have large quantum numbers: for example, $n \sim 40$. In the discussion below, we will use Cs as the example Rydberg atom because it was used in [8]. In an experiment, the quantum number $n$ can be chosen by tuning the frequency of the laser that excites the atoms to the Rydberg states.

## 2. Computational method

In this section, we describe the various parts of the calculation that determine the accuracy and applicability of our results.

### *2.1. Numerical method*

In our numerical simulation of the $e^+$ and $e^-$ classical trajectories, we utilized the adaptive step size, fourth-order Runge–Kutta time propagation scheme [10]. We checked the accuracy of each trajectory by comparing conserved quantities (e.g. total energy) at the end of the trajectory to that at the beginning. Any trajectory with a change in a conserved quantity larger than 0.01% was rejected from our sample. Our rejection rate was very low and should not affect our results; for example, only 2–3% of the trajectories that gave a charge exchange were rejected for $n = 40$ at $B = 1$ T and only for the lowest energy $e^+$ calculations. We used the full equations of motion for the light particles since it was not clear how accurate various approximations (e.g. the guiding center approximation) would be for all of the fields and energies in our calculations.

We approximated the interaction of the $Cs^+$ ion with the electron ($e^-$) and $e^+$ as being a pure Coulomb force for all distances. This is clearly a poor approximation when either the $e^-$ or $e^+$ is within $\sim 10^{-10}$ m of the nucleus. However, the number of trajectories that traverse this region is small for the highly excited states used in practice and all of the interesting physics

occurs when both light particles are far from the nucleus. Thus, we expect this approximation to be very good for the results reported below.

### 2.2. Initial distribution

We simulated the production of Ps through charge exchange from highly excited cesium (Cs) to an approaching $e^+$. In this stage, we considered the Cs nucleus as an infinitely massive, fixed body. This should be a good approximation because the $e^+$ speed is more than 10 times that of the atom; also, the motional Stark field, $vB$, for the atom is only several V cm$^{-1}$, which is less than that needed to $n$-mix states near $n \sim 40$. The Cs is in a highly excited state, but the position and velocity distribution of the highly excited $e^-$ is not known. The atom is laser excited to a specific $n\ell$ state, but travels through fields (which can mix the $\ell$ states) and then interacts with many $e^+$'s (which strongly mixes $\ell$ and more weakly mixes $n$) before a charge transfer takes place to give Ps. We have assumed that the $e^-$ on the atom is at the energy of a specific $n$-state but that the angular momentum has been randomized. Thus, we start the $e^-$ on the atom in a microcanonical ensemble at the energy of a hydrogenic $n = 40$ state. From the calculations of [9], we found that the results did not depend strongly on $n$ when going from 30 to 40 to 50 as long as the parameters were properly scaled. Thus, we expect our results to apply to other $n$ as long as the energies or temperatures are scaled by the factor $(40/n)^2$, the lengths are scaled by $(n/40)^2$ and so on.

In the first step, the $e^+$ is fired at the highly excited Cs atom. To simplify the discussions below, we will assume the magnetic field is in the $z$-direction. The $z$-position ($\vec{B} \equiv B\hat{z}$) of the $e^+$ is started 20 times the size of the atom from the nucleus, where we take the size of the atom to be $2n^2a_0$. The $x$, $y$-position of the $e^+$ was random within a square with an edge length 14 times the size of the atom. The final choice for all sizes (like 20 times the size of the atom, for example) was made by doubling the relevant parameters until the final result did not change within our statistics. The $e^+$ velocities were initialized using the Maxwell–Boltzmann distribution at a temperature, $T$, for the perpendicular velocity components. As described below, some calculations used a thermal distribution for the parallel velocity and some calculations used a fixed velocity. The propagation was terminated when the magnitude of the difference of the $z$-positions of the $e^+$ and $Cs^+$ differed by more than $\sim$50 times the size of the atom. When the $e^+$ reached this point, we determined whether or not it had captured the $e^-$ by checking the distance between the $e^+$–$e^-$. If this distance was less than three times the original atom's size, we counted this as a Ps formation; if Ps formation did not occur and the $e^-$ was more than three times the original atom's size from the $Cs^+$ ion, we counted this as an ionization. The number of Ps formed only weakly depended on the cut-off distance we used but the ionization was sensitive to this distance. We picked three times the atom size as the cut-off distance because electrons that can travel outside of this region have $n > 70$ and will be ionized when a subsequent $e^+$ hits the atom. From these initial conditions, we ran enough trials so that we obtained approximately 4 000 recombined $e^-$–$e^+$ pairs for each set of initial conditions, which is a large enough sample to obtain physical parameters to better than 10% accuracy.

The numerical value for the cross section is obtained by multiplying the area through which the $e^+$'s are launched by the fraction of trajectories that lead to a specified outcome. The collision rates for the thermal distributions of $e^+$'s are obtained by multiplying the cross section by the average speed parallel to the $B$-field, $\sqrt{2k_BT/(\pi m)}$.

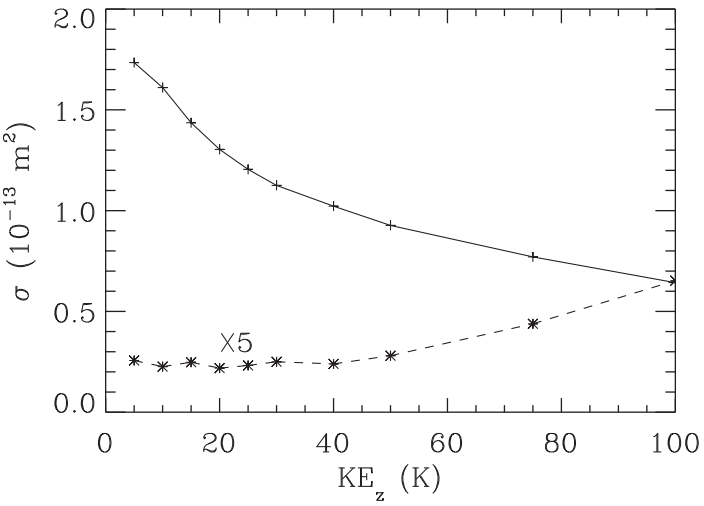


**Figure 1.** Charge exchange (solid line) and ionization (dashed line) cross sections as a function of the kinetic energy of the $e^+$ parallel to the $B$-field. The electron's initial condition is from a microcanonical ensemble at energy corresponding to the hydrogen $n = 40$ state. The $e^+$ perpendicular velocity is from a 30 K thermal distribution.

## 3. Results

We computed the statistics associated with the physical properties of the Ps formed in our simulation. We focused on the ionization and charge transfer rates and cross sections. We computed these parameters both for a fixed initial $v_z$ and for a thermal distribution of $e^+$. We also give results for the angular distribution of Ps that result from a charge transfer. Finally, we investigated how large an $E$-field the Ps could survive depending on their emergence angle.

### *3.1. Single* $e^+$ *collisions*

In this section, we investigate the cross sections and rates for the case when the atom is constrained to keep the binding energy fixed (i.e. each time an $e^+$ is fired at the atom a new set of initial conditions for the $e^-$ is generated from a microcanonical ensemble). This situation is not quite physical because the atom usually experiences several collisions before either charge transfer or ionization occurs. Thus, the binding energy will evolve while the atom is in the $e^+$ plasma. Although the situation is not directly relevant to experiments, it allows us to examine these processes in a more controlled situation. We will treat the case of multiple collisions below.

*3.1.1. Fixed* $KE_z$. Figure 1 shows the cross sections for the case where we fixed the $e^+$'s initial kinetic energy in the $z$-direction but we picked the perpendicular velocities from a thermal distribution at 30 K. Fixing the kinetic energy in the $z$-direction while having a thermal distribution in the perpendicular direction is an artificial division of the energy dependence. The reason for this choice is to show how the cross sections strongly vary with the energy along the field. This figure is for atoms with a binding energy corresponding to $n = 40$; for reference, the binding energy is 98.6 K. If we take the geometric cross section to be $\pi(2n^2a_0)^2$, then this value for $n = 40$ is $9.00 \times 10^{-14}\,\mathrm{m}^{-2}$.

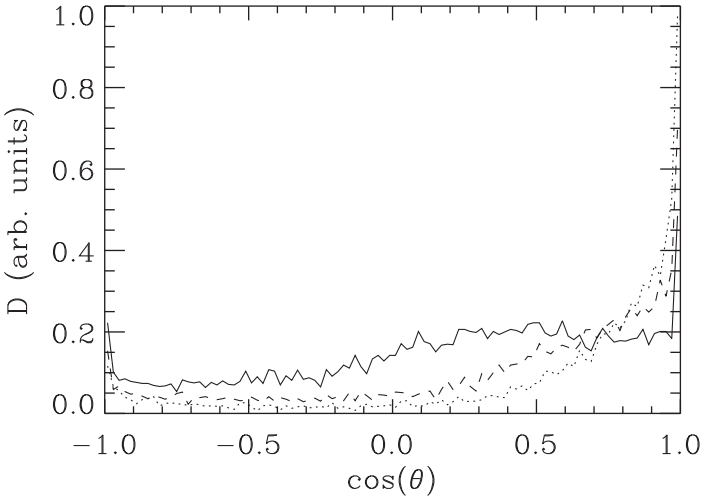


**Figure 2.** Angular distribution of the Ps formed as in figure 1: $\theta$ is the angle between the direction of the Ps and the $z$-axis. The solid line is for $KE_z = 10\,\mathrm{K}$, the dashed line is for 30 K and the dotted line is for 50 K. To emphasize the asymmetry, the $e^+$'s are all launched from negative $z$ with a positive $v_z$.

The $KE_z \to 0$ charge transfer cross section is approximately double the geometric value. The charge transfer cross section decreases monotonically over the range plotted by a factor of ∼3. This decrease is because it is more difficult for the positron to capture the electron as the energy of the positron increases; the charge transfer mainly occurs when the incoming particle has speed comparable to or less than that of the electron. The ionization cross section increases with energy over the range plotted because increasing the positron energy will give more positrons with sufficient energy to ionize the atom. It might be a surprise that positrons with parallel energy much less than the 98.6 K binding energy can cause ionization; this is allowed because the thermal distribution of the perpendicular kinetic energy can, in some cases, supply the extra energy needed for ionization. For the $KE_z = 100\,\mathrm{K}$ case, the ionization cross section is approximately 1/5 of the charge transfer cross section, giving a branching ratio of ∼1/6 for ionization. At higher energies than plotted here, the ionization cross section reaches a maximum and then decreases. The decrease at higher energy is due to the usual decrease in the Coulomb cross section with increasing energy.

Figure 2 shows the angular distribution of the Ps for three $KE_z$. We have plotted the results versus $\cos(\theta)$ because that will account for the phase space weight of different angles; an isotropic distribution will give a flat distribution in $\cos(\theta)$. To see the largest possible effect, we have launched all of the positrons at large, negative $z$ with a positive $v_z$ for this graph. In a plasma, equal numbers of positrons will have positive and negative $v_z$ because there is no net flow of positrons along the magnetic field: there must be equal numbers of $e^+$ approaching the atom from positive $z$ with a negative $v_z$ as approaching the atom from negative $z$ with a positive $v_z$. This leads to a symmetric distribution in $\cos(\theta)$. Unlike the results in figure 1 [9], the angular distribution is clearly not isotropic.

In all cases, there is a sharp peak in the forward direction and a much smaller sharp peak in the backward direction. The relative size of the peak increases as $KE_z$ increases. This is due to the capture of the electron by relatively large impact parameter $e^+$'s. The Ps with $\cos(\theta) \simeq 1$

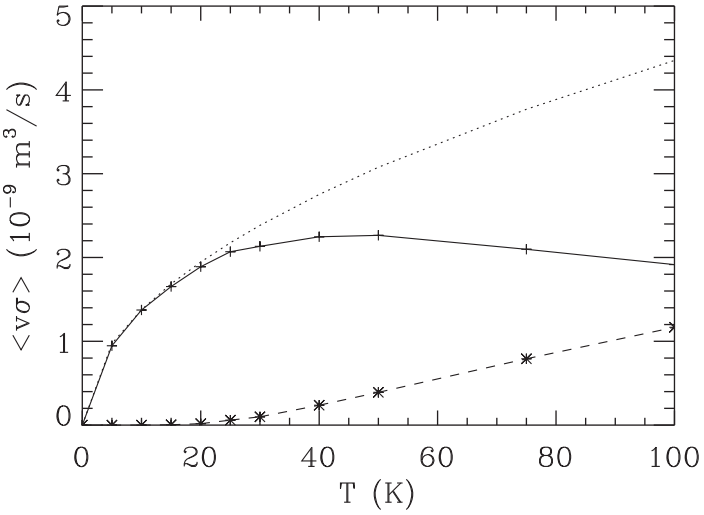


**Figure 3.** Charge exchange (solid line) and ionization (dashed line) rates as a function of the temperature of the $e^+$. The electron's initial condition is from a microcanonical ensemble at energy corresponding to the hydrogen $n = 40$ state. The dotted line is the result from equation (1) with $C = 3.9$.

have a larger fraction of cases with weak binding (we will see this below when we look at how electric fields can destroy the Ps). The sharp peak in the forward direction will be decreased by a factor of ∼2 when accounting for the fact that the $e^+$ can hit the atom with positive or negative $v_z$. Although Ps with $\cos(\theta) \simeq 1$ are more easily destroyed by electric fields, the peak is good news with regard to using the Ps for making $\bar{H}$'s because more of the $\bar{p}$'s will be in the direction $\cos(\theta) \sim 1$. Although the result does not correspond directly to a physically relevant situation, we could compute the number of Ps in the region $0.98 \leqslant |\cos(\theta)| \leqslant 1$ and found that the $KE_z = 10\,\mathrm{K}$ case had an enhancement by a factor of 2.5 from isotropic, 30 K had an enhancement by a factor of 4.3 and 50 K had an enhancement by a factor of 6.6.

*3.1.2. Thermal $KE_z$.* Figure 3 shows the rate for charge transfer and ionization processes versus the temperature of the positrons. For this case, the parallel velocity is chosen from a distribution proportional to $v_z \exp(-mv_z^2/[2k_BT])$ with the factor $v_z$ giving the proper Maxwell–Boltzmann distribution in $z$ and the perpendicular velocity is chosen from a thermal distribution at the same temperature. The dotted line uses the form from equation (2) with $C = 3.9$. At temperatures below ∼20 K, our results agree well with the finding in [9], but at higher temperatures, our rate is well below the form which was obtained for temperatures of 4 or 8 K. This difference is due to the fact that higher-temperature positrons have speeds higher than the electron in the atom so that it is harder for the positron to capture an electron. Also, the ionization rate increases as the positron temperature increases. Thus, competition with the ionization process also decreases the charge transfer cross section. In the previous section, the branching ratio for ionization was ∼1/6 at 100 K. For the thermal distribution, the branching ratio is ∼2/5 at 100 K. The branching ratio for ionization at 100 K has substantially increased because the average $e^+$ energy for the thermal case is almost twice as large as the figure 1 case at 100 K. Finally, there is almost no ionization in figure 3 below ∼20 K because there are almost no positrons in the distribution with sufficient energy to ionize $n = 40$; in figure 1 there was

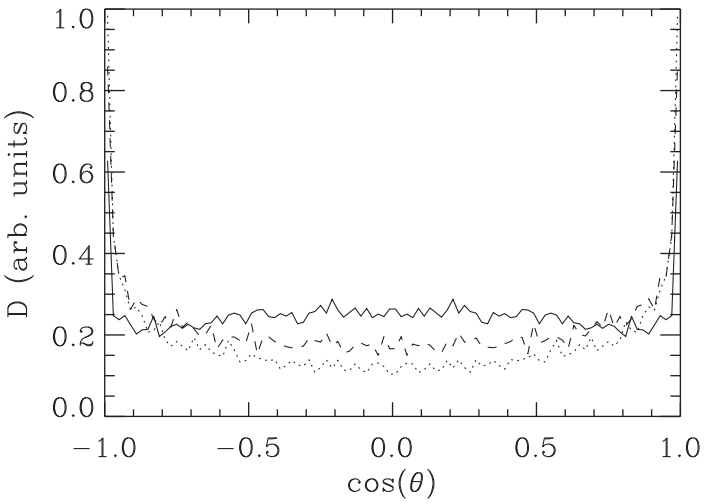


**Figure 4.** The same as figure 2 but for a thermal positron distribution; the solid line is for $T = 10$ K, the dashed line is for 30 K and the dotted line is for 50 K. As in a plasma, the $e^+$ are fired at the atom with positive and negative $v_z$, which leads to a symmetric distribution.

ionization for $KE_z < 20$ K because the 30 K perpendicular velocity distribution could supply the energy for ionization.

Figure 4 shows the angular distribution of the Ps formed for temperatures of 10, 30 and 50 K. Unlike figure 2, this distribution is symmetric about the value $\cos(\theta) = 0$ because the $e^+$ are fired at the atom with both positive and negative $v_z$. The angular distribution is approximately flat except for the angular bin extending from 0.98 to 1. The number of Ps in the region $0.98 \leqslant \cos(\theta) \leqslant 1$ for 10 K $e^+$ had an enhancement by a factor of 2.5 from isotropic, 30 K had an enhancement by a factor of 3.9, and 50 K had an enhancement by a factor of 5.4. This figure shows that the peak in the forward direction still exists for the more realistic case of thermal $e^+$.

### *3.2. Multiple* $e^+$ *collisions*

The information in the previous sections is useful in gaining insight into how the charge exchange and ionization processes depend on the energy or temperature of the $e^+$. However, this information, by itself, is not quantitatively relevant for computing the useful parameters for an experiment like [8]. The reason is that the largest cross section for a $e^+$ hitting a Rydberg atom is for angular momentum or binding energy change. There will be several $e^+$ collisions with the Rydberg atom before a charge exchange or ionization takes place. The binding energy could substantially change, which could lead to a substantial change in the branching ratio between ionization and charge transfer. Also, the properties of the Ps formed by the charge transfer might be substantially different. In a few cases (less than 0.1%), the atom becomes so deeply bound that we stop the simulation and count it as a cascade to the ground state.

For the calculations in this section, the $e^+$'s velocity is randomly chosen from a thermal velocity distribution as in section 3.1.2. Instead of having a new atomic trajectory for each time we launch an $e^+$, we do not re-initialize the electron's parameters until either ionization or charge transfer has occurred. In practice, we start the simulation by picking the electron's

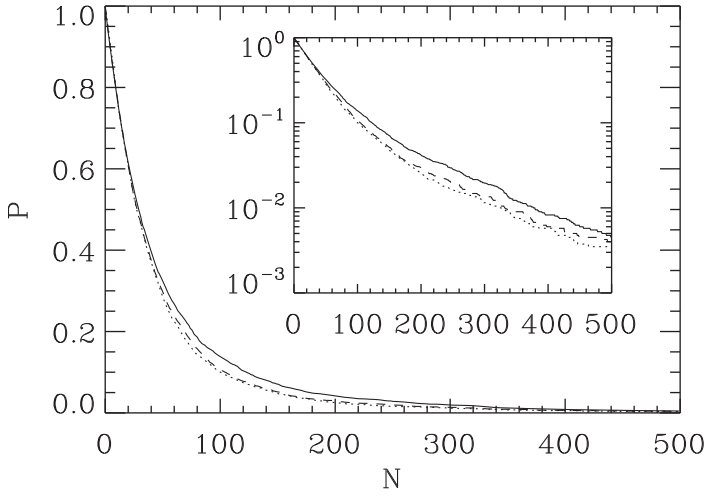


**Figure 5.** The atom's survival probability as a function of the number of $e^+$'s fired at it. The electron's position and velocity are *not* re-initialized after each $e^+$. The solid line is for $T = 10$ K, the dashed line is for 30 K and the dotted line is for 50 K.

initial position and velocity from a microcanonical ensemble. We then fire a $e^+$ at the atom. If neither ionization nor charge transfer occurs, we fire another $e^+$ at the atom using the electron's position and velocity from the time when the first $e^+$ reached a distance ∼50 times the atom size from the $Cs^+$. We repeated this (in some cases for thousands of $e^+$) until ionization or charge transfer occurred. We found that it was not necessary to let the electron in the Rydberg atom evolve for random times between $e^+$ collisions; this is because the region for strong interactions is approximately two times the atom size so that all of the time the $e^+$ takes to reach 50 times the atom size gives a random amount of time for the electron to evolve *and* because most of the $e^+$ have too large an impact parameter to strongly affect the atom, so the whole of the calculation time for such a $e^+$ is basically unperturbed evolution for the atom.

Figure 5 shows the survival probability of the atom after $N e^+$'s have been fired at the atom for $e^+$ temperatures of 10, 30 and 50 K. The $x$-axis is the number of $e^+$ that have been fired at the atom which would be proportional to the time the atom is in the $e^+$ plasma and the plasma temperature and density. The survival probability depends on $N$ through both trivial factors (e.g. if we change the size of the square from which we pick the $e^+$ initial $xy$-position, then the survival probability decreases more slowly with $N$ as we make the square bigger) and important factors (e.g. the survival probability decreases more quickly if the cross sections are larger). Since there is a similar decay curve for different temperatures, this implies that the rate will scale as $\sqrt{T}$, as seen in figure 3. At early times, there is a rapid decay of the survival probability with a rate that approximately equals the sum of the ionization and charge transfer rates for $n = 40$. At later times, there is a noticeable slowing of the rate as seen in the inset. This is because some collisions will leave the atom more deeply bound. More deeply bound atoms are destroyed by ionization or charge transfer more slowly because the geometric cross section scales with the inverse of the squared binding energy.

Figure 6 depicts a more important consequence of the evolution of the atom due to multiple $e^+$ collisions. This figure shows the branching ratio for ionization versus the temperature of the $e^+$'s. The case when we do not allow the atom to evolve gives a branching ratio for

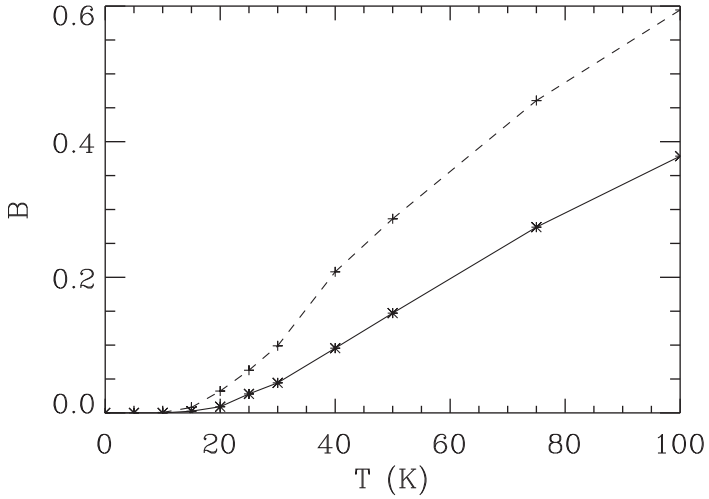


**Figure 6.** Branching ratio for ionization as a function of the $e^+$ temperature. The solid line is when the electron's position and velocity are re-initialized for each $e^+$ launched at the atom and the dashed line is when the electron is *not* re-initialized.

ionization that is substantially less than that for the case when we allow the atom to evolve. This is understandable, because the binding energy often substantially decreases in the multiple collision case before the atom is destroyed. For example, in the 30 K case, we found that the atoms that ionized mostly had a binding energy (just before the launch of the $e^+$ that destroyed the atom) substantially less than the original binding energy.

### *3.3. Multiple* $e^+$ *collisions, E-field*

We used the Ps formed in the previous section and applied to them an increasing electric field. A strong enough $E$-field will pull the Ps into a free $e^+$ and $e^-$. This situation is relevant because the plasmas in the anti-hydrogen experiments are held in place using electric fields. The size of the $E$-fields depends on the number of positrons or $\bar{p}$'s being held and in how small a spatial region they are held. We expect that the maximum $E$-field in the path between the positron plasma (where the Ps is formed by charge exchange) and the $\bar{p}$ plasma (where the second charge exchange will make an $\bar{H}$) will be between several tens $V\,cm^{-1}$ to a couple of hundred $V\,cm^{-1}$. For all calculations in this section, we use a $e^+$ temperature of 30 K although we have performed calculations for 10 and 50 K as well. We tested several ramp rates and found that the results were independent of ramp rate as long as we ramped the electric field slower than $(27.21\text{V})/(a_0 n^4)$ per $(250 n^3 \text{fs})$.

There are two important consequences of the Ps getting destroyed in an $E$-field. The first is that an $\bar{H}$ will not be formed if the Ps was traveling directly toward the $\bar{p}$ plasma, but will be destroyed before reaching it. The second is that a Ps that would have missed the $\bar{p}$ plasma might get destroyed close enough to the $e^+$ plasma so that the positron goes back into the plasma and can be re-used for another charge exchange.

Donnan *et al* [11] computed the ionization of an atom in a strong magnetic field by a rising electric field. Their figure 2 shows the result for $n = 30$ and a 1 T magnetic field. The atom ionizes between 800 and $1600\,V\,cm^{-1}$. If we scale these fields by a factor of $(30/40)^4$,

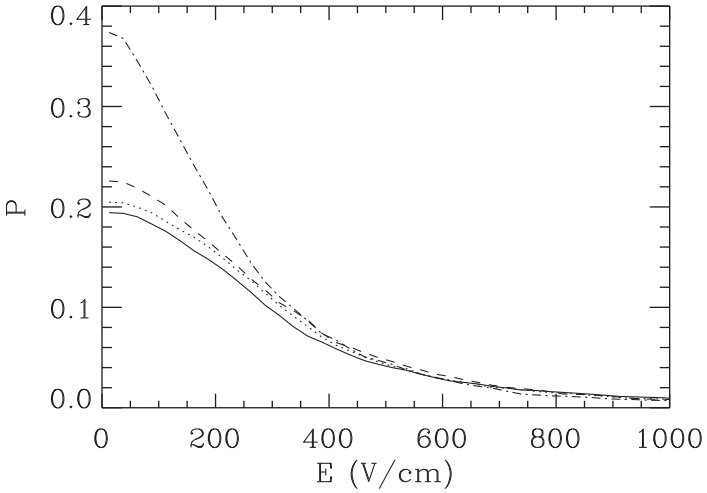


**Figure 7.** Probability that a Ps is in each of the regions $0 \leqslant |\cos(\theta)| \leqslant 1/4$ (solid line), $1/4 \leqslant |\cos(\theta)| \leqslant 1/2$ (dotted line), $1/2 \leqslant |\cos(\theta)| \leqslant 3/4$ (dashed line) and $3/4 \leqslant |\cos(\theta)| \leqslant 1$ (dot-dashed line) *and* survives an electric field, $E$, parallel to the magnetic field. The electron's position and velocity are *not* re-initialized after each $e^+$.

we expect the relevant electric fields where the atom will ionize to range between 250 and 500 V cm$^{-1}$.

Figure 7 shows the survival probability as a function of maximum $E$-field where the electric and magnetic fields are parallel to each other. The four different curves show the probability for a Ps to be emitted into different angular ranges ($|\cos(\theta)|$ between 0 and 1/4, between 1/4 and 1/2, between 1/2 and 3/4 and between 3/4 and 1) *and* survive a maximum $E$-field. Figure 8 shows the survival probability but for the case when the electric and magnetic fields are nearly perpendicular to each other.

There are several important features of these figures. Firstly, the survival probability at $E = 0$ gives the probability for the Ps to be emitted in four different angular ranges. Secondly, the main drop in the survival probability is spread over a larger range of $E$-fields than would be expected from the paper [11]; this is because the Ps that are formed have a variation in their binding energy and Ps with larger/weaker binding energy can survive stronger/weaker fields. Thirdly, the Ps that are in the range $3/4 \leqslant |\cos(\theta)| \leqslant 1$ (the Ps traveling most nearly in the $z$-direction) are destroyed by weaker electric fields on average; this is because the more weakly bound atoms are correlated with traveling in the $z$-direction. Fourthly, there is not much difference between having the electric field parallel or nearly perpendicular to the magnetic field for fields greater than $\sim$300 V cm$^{-1}$; the biggest difference is for electric fields less than 200 V cm$^{-1}$ where the perpendicular case has almost all atoms surviving, whereas the parallel case loses $\sim 1/4$ of the atoms for $|\cos(\theta)| \leqslant 3/4$ and loses $\sim 1/2$ of the atoms for $|\cos(\theta)| \geqslant 3/4$. Fifthly, we found that a much larger electric field is needed to destroy the Ps if the electric and magnetic fields were exactly perpendicular; more than 1/2 of the Ps could survive electric fields of $\sim$1500 V cm$^{-1}$ for the exactly perpendicular case.

Taken together, these figures have important implications for how the Ps behaves in the anti-hydrogen experiments. The Ps that will travel to the $\bar{p}$ plasma (where the second charge

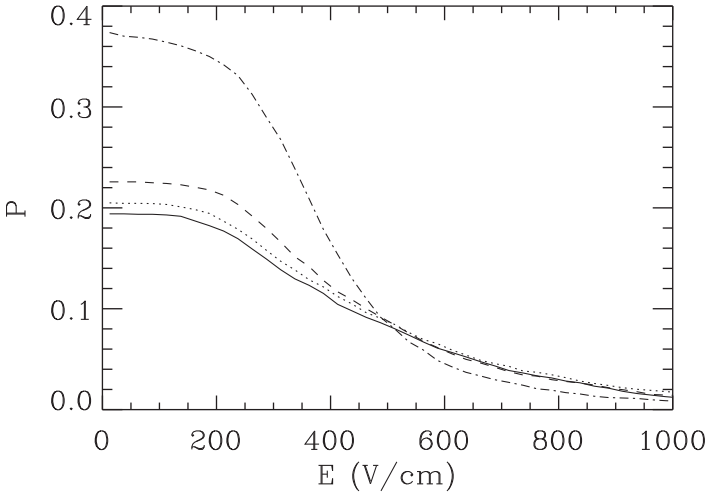


**Figure 8.** The same as figure 7 but for an electric field nearly perpendicular to the magnetic field. We chose $\hat{E} \cdot \hat{B} = 0.1$, which is an angle of $84.3^{\circ}$ between the electric and magnetic fields.

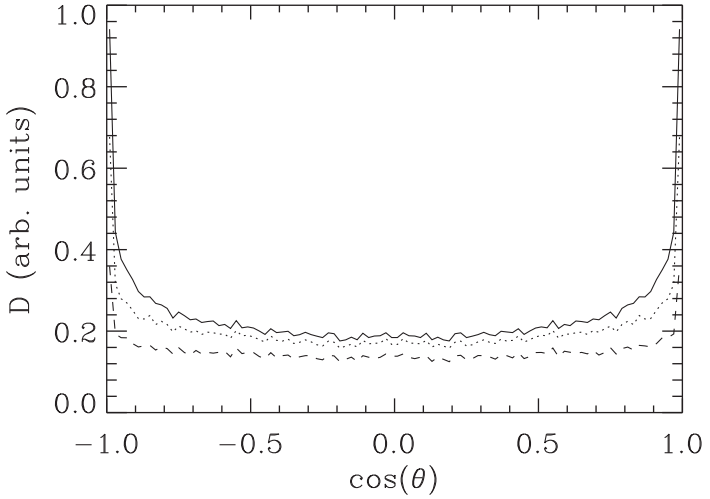


**Figure 9.** Angular distribution for Ps that survive an electric field of $0\,\mathrm{V\,cm^{-1}}$ (solid line), $100\,\mathrm{V\,cm^{-1}}$ (dotted line) and $200\,\mathrm{V\,cm^{-1}}$ (dashed line). The $e^+$'s have a temperature of 30 K and the electron's position and velocity are *not* re-initialized for each $e^+$ launch. The electric field is parallel to the magnetic field.

exchange will make an $\bar{H}$) will be traveling along the trap axis and will experience electric fields nearly parallel to the magnetic field. Thus, the $|\cos(\theta)| \geqslant 3/4$ in figure 7 is most relevant for determining the probability for a Ps to reach the $\bar{p}$ plasma. The Ps that travel to the side will experience a very large electric field inside the $e^+$ plasma which will be perpendicular to the magnetic field. Once outside the plasma, the Ps will experience only a small electric field parallel to the magnetic field due to the symmetry of the electric potential in $z$. Thus, the curves with $|\cos(\theta)| \leqslant 3/4$ in figure 8 are most relevant for determining whether a Ps gets stripped early enough for the $e^+$ to return to the $e^+$ plasma. This suggests that unless the electric field gets above $200\,\mathrm{V\,cm^{-1}}$ almost *all* of the Ps will move too far from the plasma for the $e^+$ to return.

Finally, figure 9 shows the angular distribution of the Ps that survive a parallel electric field of 0, 100 or 200 V cm$^{-1}$. The 0 V cm$^{-1}$ case is similar to that in figure 4 but for multiple $e^+$ interactions with the atom. The curve for the Ps that survive a 100 V cm$^{-1}$ field hardly decreases from the 0 V cm$^{-1}$ case except for near the $\cos(\theta) \sim \pm 1$. The 200 V cm$^{-1}$ survivors have become even flatter; the $\cos(\theta) \sim \pm 1$ decreases by a factor of ~2.5, whereas the $\cos(\theta) \sim 0$ decreases by ~30%. This figure clearly shows that the Ps that travel along the magnetic field are more strongly affected by electric fields than those that move perpendicular to the magnetic field. In spite of this effect, there is an enhancement for $\cos(\theta) \sim \pm 1$ which will benefit the experiments attempting to trap anti-hydrogen.

## 4. Conclusions

We have calculated the charge exchange and ionization that occurs when a Rydberg atom is in a $e^+$ plasma. We found that the higher temperatures compared to those examined in [7, 9] strongly affect the expected properties of the Ps formed. Our calculations were performed for a magnetic field of 1 T and for a range of $e^+$ temperatures that seemed reasonable for the present experiments. We found that there is a tendency for the Ps to travel parallel to the magnetic field and this will, thus, enhance the possibility of a second charge transfer in experiments such as [8].

In addition to looking at total cross sections and rates, we examined how big an electric field the Ps could survive. We found that the angle that the Ps travels relative to the magnetic field has an effect on the size of the electric field it could survive. The dependence is non-intuitive since the atoms that are most easily destroyed are those moving nearly parallel to the magnetic field, which are the ones with the *least* motional electric field, $\vec{v} \times \vec{B}$.

The results presented in this paper can be used to estimate the parameters needed to successfully trap anti-hydrogen made from this two-stage charge exchange. For example, calculations of state-selective field ionization of atoms predict that fields less than ~250 V cm$^{-1}$ will not strip $n = 40$ atoms; however, figure 9 shows that the propensity to make weakly bound Ps leads to a strong decrease of Ps in the $\cos(\theta) \sim 1$ direction for an electric field of 200 V cm$^{-1}$. We also found that the Ps that move nearly perpendicular to the magnetic field are destroyed at higher fields and, thus, the $e^+$ probably are not going to return to the $e^+$ plasma. Finally, as a basic question about atomic processes, this system once again shows that non-intuitive behavior seems to be the likely outcome for Rydberg atoms in strong magnetic fields.

## Acknowledgments

This work was supported by the Chemical Sciences, Geosciences, and Biosciences Division of the Office of Basic Energy Sciences, US Department of Energy. This work was made possible in part by a grant of high-performance computing resources and technical support from the Alabama Supercomputer Authority.

## References

[1] Andresen G B *et al* (ALPHA Collaboration) 2010 *Nature* **468** 673
[2] Andresen G B *et al* (ALPHA Collaboration) 2011 *Nature Phys.* **7** 558
[3] Andresen G B *et al* (ALPHA Collaboration) 2011 *Phys. Rev. Lett.* **106** 025002
[4] Gabrielse G, Rolston S L, Haarsma L and Kells W 1988 *Phys. Lett.* A **129** 38

[5] Glinsky M E and O'Neil T M 1991 *Phys. Fluids* B **3** 1279
[6] Robicheaux F and Hanson J D 2004 *Phys. Rev.* A **69** 010701
[7] Hessels E A, Homan D M and Cavagnero M J 1998 *Phys. Rev.* A **57** 1668
[8] Storry C H *et al* 2004 *Phys. Rev. Lett.* **93** 263401
[9] Wall M L, Norton C S and Robicheaux F 2005 *Phys. Rev.* A **72** 052702
[10] Press W H, Teukolsky S A, Vetterling W T and Flannery B P 1992 *Numerical Recipes* 2nd edn (New York: Cambridge University Press)
[11] Donnan P H, Niffenegger K, Topcu T and Robicheaux F 2011 *J. Phys. B: At. Mol. Opt. Phys.* **44** 184003